

Deep Learning based Anomaly Detection

Le Sun^{1*}, Jinyuan He², Xiaoxia Yin², Yanchun Zhang², Jeon-Hor Chen^{3,4},
Tomas Kron⁵, Min-Ying Su³



¹ School of Computer and Software, Nanjing University of Information Science and Technology,
Nanjing, Jiangsu, China
sunle2009@gmail.com

² Centre for Applied Informatics, Victoria University, VIC, Australia
jinyuan.he@live.vu.edu.au, {xiaoxia.yin, yanchun.zhang}@vu.edu.au

³ Department of Radiological Sciences, University of California, Irvine, CA, USA

⁴ Department of Radiology, E-Da Hospital and I-Shou University, Kaohsiung, Taiwan
{Jeonhc,msu}@uci.edu

⁵ Peter MacCallum Cancer Centre, VIC, Australia
Tomas.Kron@petermac.org

Received 9 January 2018; Revised 17 January 2018; Accepted 22 January 2018

Abstract. Magnetic resonance imaging (MRI) has been a prevalence technique for breast cancer diagnosis. This paper introduces a semi-supervised method for extracting breast tumors in a set of real MRIs of different types of breast cancer patients. We call the proposed method as Semi-supervised Tumor Segmentation (SSTS), and apply it to both mass and non-mass lesions. We have trained 225 classifiers with respect to different settings of threshold parameters that need to be set in SSTS. We will show the performance of SSTS for extracting the infiltrating ductal carcinoma (IDC) and the ductal carcinoma in situ (DCIS) tumors based on a set of real MRIs of 21 breast cancer patients; and how different settings of the parameters will influence the extraction results. We additionally implement five state-of-the-art intensity-based image segmentation algorithms that can be compared with SSTS on breast tumor extraction.

Keywords: breast tumor, image segmentation, MRI, semi-supervised learning

1 Introduction

Breast cancer is one of the most common cancer that causes deaths in women worldwide [1]. Magnetic resonance imaging (MRI) is an advantageous technique for breast cancer diagnosis. Radiologists assess MRIs slice-by-slice to locate lesions and diagnose diseases, which is an arduous and time-consuming task in real clinical applications [2]. Therefore, computer-aided detection and segmentation of lesions from

MRIs plays an increasing vital role for breast cancer diagnosis.

Numbers of researchers focused on lesion segmentation in MRIs in past decades [3-4]. Issues in the state-of-the-art breast tumor extraction methods include (1) some methods require manual delineation of ROIs as a step of initialization (e.g. [5]), which restricts the automatic segmentation to cases that sufficient expert knowledge should be known in advance [6]; (2) supervised methods require a large amount of labelled images for model construction or parameter learning (e.g. [6]); (3) existing work mainly focuses on segmenting mass tumors (e.g. [2-3, 6]), less investigation on segmenting non-mass lesions because of the shape diversity of the lesions.

To tackle these issues, we propose an unsupervised method for breast tumor segmentation, and take a

* Corresponding Author

supervised classification step to classify the tumor and non-tumor pieces obtained from the unsupervised segmentation to automatically locate the tumor regions in an MRI. We call the proposed method as Semi-supervised Tumor Segmentation (SSTS), which comprises four main steps (Fig. 1 modules 1-4): at first, we segment an imaged MRI by using Otsu thresholding [7]; and then remove the cluster in low intensity levels, as tumors in MRI images normally have relatively high intensities. Our experiment results show this thresholding step can dramatically improve the performance of super-pixel segmentation of module 2. Secondly, over-segment the remaining image based on the Simple Linear Iterative Clustering (SLIC) method [8] to form super-pixels, which further reduces the number of pixels and improves the clustering efficiency in the sequel stages. Thirdly, group super-pixels based on the DBSCAN technique [8] in terms of mean intensities and positions of super-pixels. Finally, classify tumor pieces to locate tumors in the original image by using an Adaboost classification algorithm [9] based on 20 texture features [5].

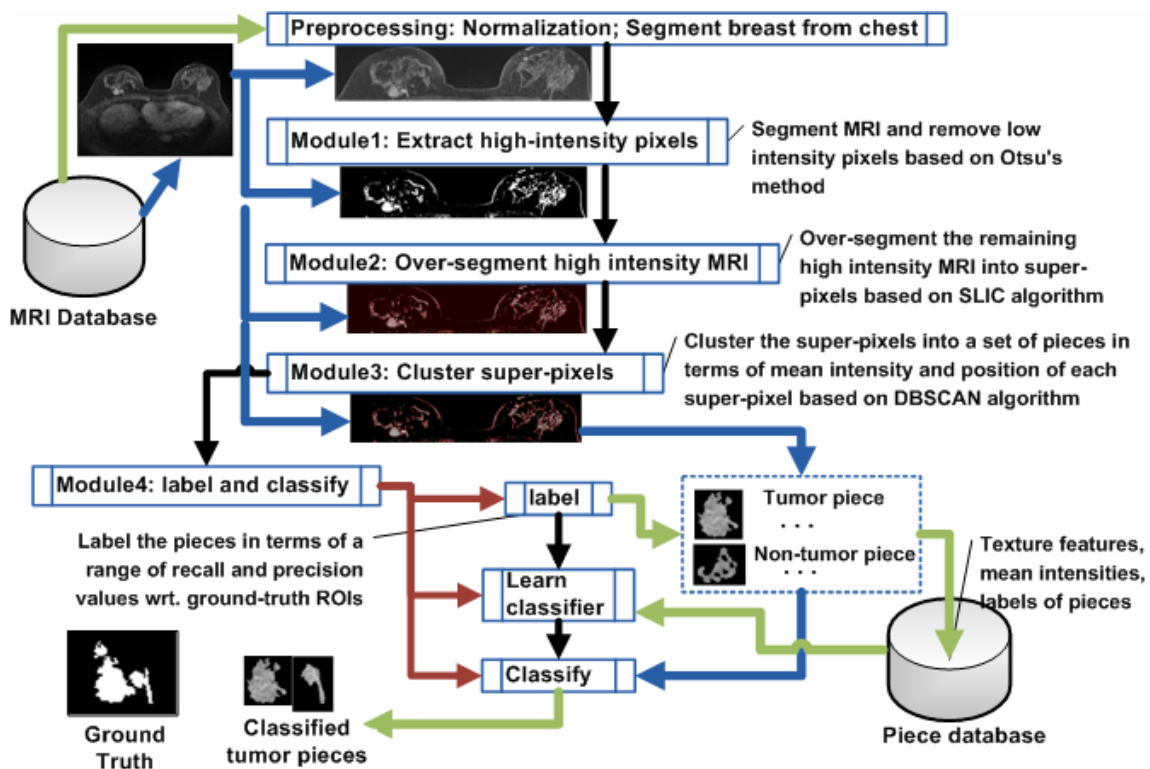


Fig. 1. Overview of Semi-supervised tumor segmentation framework (SSTS)

To obtain the optimal performance of tumor extraction, we take extensive experiments to learn parameters of segmenting and classifying (Modules 2-4) and train 225 classifiers (Module5) corresponding to different parameter settings. In addition, we implement a series of intensity-based tumor segmentation algorithms, including Particle Swarm Optimization (PSO) [10], Fractional-order Darwinian Particle Swarm Optimization (FO-DPSO) [11], K-means [12], Fuzzy-C-Means (FCM) [13], and Multi-thresholding (MT) [14]. Other than intensity, we analyse texture features of breast tumors in MRIs to evaluate how different texture features assist identifying infiltrating ductal carcinoma (IDC) and ductal carcinoma in situ (DCIS) tumors. The texture features include the statistical moments (first-order and second order) [15] and 21 gray-level co-occurrence metric (GLCM) features [16].

The main contributions of our work are: (1) we design a semi-supervised method for delineating breast tumors in MRIs, which requires smaller labelled datasets compared with the full supervised methods; (2) our experiment is based on a set of real three-dimensional MRIs of 21 patients; and abundant experimental results show better performance of our work compared with the existing image segmentation techniques, e.g. a multi-threshold method (MT) [7] and a Fuzzy C Means (FCM) method [13].

The structure of this paper is: Section 2 discusses the related work; Section 3 presents the SSTS framework and its performance; Section 4 concludes this paper and discusses future work.

2 Related Work

There are mainly four types of image segmentation methods [11]: threshold-based [17-18], clustering-based [19-20], region-based [21-22], and texture analysis based [23-24]. We review the application of image segmentation techniques in the area of breast and brain tumor segmentation in this section.

Supervised learning methods are normally used for classification of different types of tumors [25-26]. Sauwen et al. [27] compared the performance of unsupervised classification algorithms for the segmentation of high-grade gliomas based on multi-parametric MRI modalities including conventional MRI, diffusion-weighted imaging, magnetic resonance spectroscopic imaging, and perfusion-weighted imaging. Unsupervised methods like Fuzzy C Means (FCM) and Particle Swarm Optimization (PSO) have been applied to brain tumor segmentation. Sehgal et al. [28] proposed an automatic method to segment brain tumors from MRIs. The method includes five steps: Image Acquisition, Pre-processing, Segmentation using FCM technique, Tumor Extraction and Evaluation.

The work on breast tumor segmentation is relatively less than the work on brain tumor segmentation. Chen et al. [29] proposed a fuzzy c-means (FCM) clustering-based method to segment breast lesions from three dimensional contrast enhanced MR images. The drawback of this method is its requirement of manually drawing ROIs as an initialization step. The authors of [6] developed a multichannel Markov random fields (MRFs) framework, in which they use conditional mutual information to search for conditional independent features. This method requires a large amount of labelled data as a priori for model construction, and it does not analyse the segmentation results on non-mass tumors by using the proposed method.

There are several significant work focusing on anomaly detection in different types of images. Li et al. [30] introduced a detection scheme for identifying the copy-move forgery in images based on the techniques of key-point extraction and the Expectation-Maximization algorithms. Zheng et al. [31] designed two algorithms: generalized fuzzy-c-means (FCM) and hierarchical fuzzy-c-means to solve the problems of the sensitivity of FCM's robustness and Euclidean distance to noise and outliers.

3 SSTS Framework Description

Fig. 1 shows an overview of SSTS. Pre-processing module is to normalise MRIs after breast separation from chests using simple image processing operation. As shown in Fig. 1, Module1 segments the breast MRI based on the Otsu thresholding [7] of imaged intensity. As imaged tumors in MRIs normally show high intensity levels, the clustered pixels with low intensity are removed. The remaining high intensity parts are over-segmented to super-pixels using SLIC [8] (Module2). Our work has empirically shown that the thresholding step can improve the efficiency of the over-segmentation by removing low intensity noise. Module3 clusters super-pixels based on the DBSCAN technique [8] in terms of mean intensities and positions. As a lesion is normally presented as a connected area in an MRI, this step groups super-pixels having similar intensity, and meanwhile are spatially adjacent (according to 8-adjacency matrix) to each other.

After DBSCAN clustering (Module4), we get a set of tumor and non-tumor patches, where a (non-) tumor patch means a patch is part of a (non-)tumor area or covers a (non-)tumor area (see Fig. 1). As the patches cannot always fit the real tumor area well, we define: if the area of a patch coinciding with the ground truth tumor area is above a threshold (r), it is a tumor patch. We use the dice ratio (DR) between a patch and a ground truth to measure the coinciding area of tumor and non-tumor patches.

Each labelled patch (tumor/non-tumor) is described by 21 features (20 texture features and mean intensity). The texture features [32] are defined based on the GLCM, including: *autocorrelation*, *contrast*, *correlation*, *cluster prominence*, *cluster shade*, *dissimilarity*, *energy*, *entropy*, *homogeneity*, *maximum probability*, *sum of squares: variance-sum average*, *sum variance*, *sum entropy*, *difference variance*, *difference entropy*, *information measure of correlation1*, *information measure of correlation2*, *inverse difference normalized*, and *inverse difference moment normalized*. The features of each patch are stored in the Patch database.

An Adaboost classifier [33] is trained for patch classification based on the labelled patches and their features in Patch database. The classified patches are combined together to form a tumor area in an MRI.

3.1 Parameter Setting Procedure

There are three parameters that need to be set by users in SSTS, which are distance threshold s for SLIC oversegmentation, distance threshold d for clustering super-pixels to form patches based on DBSCAN, and r for patch labelling (see Fig. 2). Values of s and d determine the clustering performance of SLIC and DBSCAN, and hence influence the extent of the segmented tumor patches fitting to the ground truth. Therefore, it is vital to carefully set values of s and d . We adopt an exhaustive method based on extensive experiments to observe the performance in terms of pre-defined values of s and d . As the performance of tumor extraction is also based on the patch classification results (i.e. whether patches are grouped to the right categories), training an efficient classifier plays a key role. Correctly labelling the segmented patches (*tumor* or *non-tumor*) is the base of the classifier training. Threshold r is defined for patch labelling.

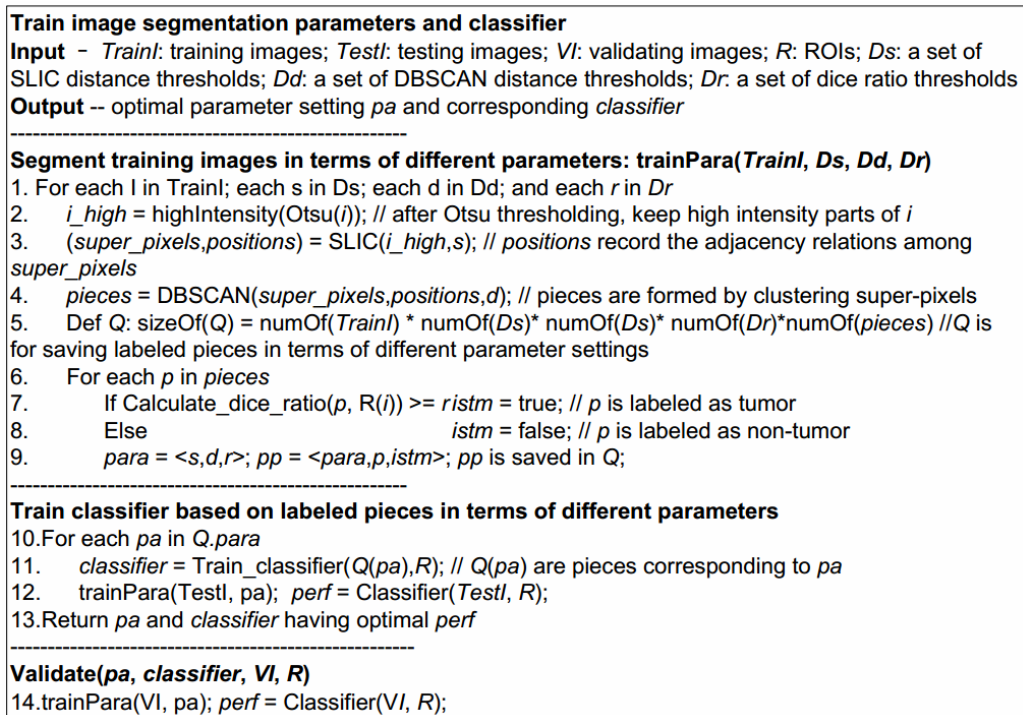


Fig. 2. Determine optimal parameters for segmenting and classifying tumor patches

The parameter training procedure is shown in Fig. 2. We separate the overall MRIs to three sets: training, testing and validating. Given an MRI i , if the DR between one patch p of i and the ground truth of i is no less than r , then p is labeled as *tumor* (see lines 7-8 in Fig. 2). Given different values of s and d , the patches of segmenting i is different. And given different r , the labelling results of patches are different. Therefore, for each patch in a segmentation, we save this patch and its corresponding parameters (s , d and r) in Q (line 9). Each setting $\langle s, d, r \rangle$ corresponds to a set of labelled patches obtained from segmenting different MRIs. For each setting, we train a classifier based on its labelled patches (line 11). We validate the performance of the classifier based on the labelled patches of *testI* (line 12). At last, we use the validation set *VI* to validate the trained parameters pa and its corresponding classifier (line 14).

3.2 Dataset Description and Empirical Parameter Setting

Our dataset includes a set of 3D MRI records of 21 patients. Each MRI image is in uint8 format, and image size is $512 * 512 * 1$ pixels. Fourteen patients have mass tumors (M), and 7 have non-mass tumors (NM). Fourteen patients have infiltrating ductal carcinoma (IDC) tumor, two have the ductal carcinoma in situ (DCIS), and five have both IDC and DCIS. The total number of MRI layers containing tumors is 407.

For each MRI layer containing tumors, we set a series of parameter values to train corresponding

tumor extraction models (*inputs* in Fig. 2), which are: $D_s = \langle 5, 10, 15, 20, 25 \rangle$, $D_d = \langle 3, 5, 8, 10, 15 \rangle$, and $D_r = \langle 0.1, 0.2, \dots, 0.9 \rangle$. For each setting of parameters, we train one classifier based on the segmented patches. Each parameter setting corresponds to around 500 tumor patches and 4000 non-tumor patches. To resolve the problem of data unbalancing, we use SMOTE method [34] to generate synthetic tumor samples, and use under-sampling method to reduce the non-tumor patches. Overall, we have 225 classifiers with respect to different parameter combinations. Users can set other parameter values to see corresponding extraction results (Fig. 3). The trained classifiers can also be used for detecting which breast (right or left) contains tumors in an MRI.

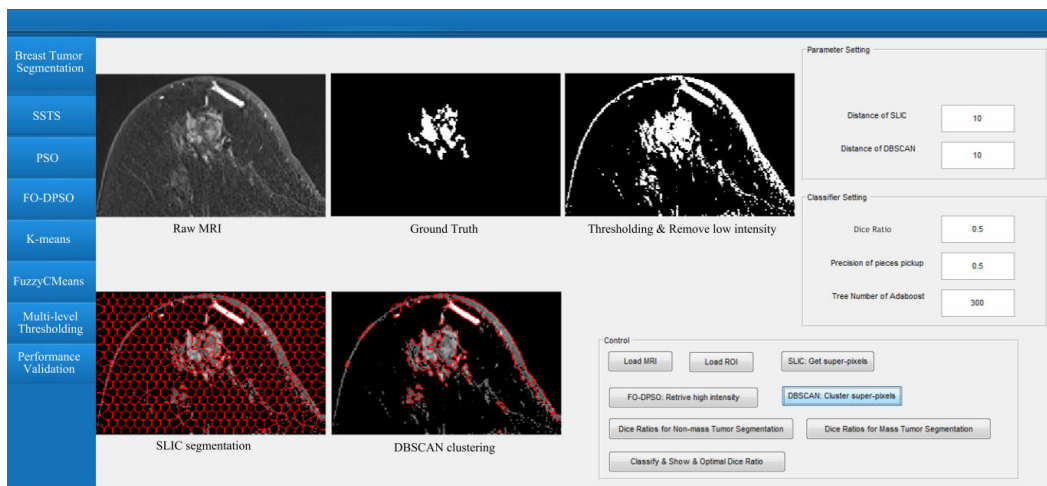


Fig. 3. Screenshot of an MRI segmentation process of SSTS. Users of the system can change parameter settings to see different segmentation results. The DB-patches are classified by a pre-trained classifier with respect to a parameter setting (e.g. $s = 10$, $d = 10$, $r = 0.5$)

3.3 Validation of Tumor Extraction

The proposed system uses both quantitative and qualitative methods to validate the performance of tumor extraction. System users can qualitatively compare the extracted tumor area (S) and the ground truth ROIs (G) (Fig. 4). Fig. 5 and Fig. 6 show the tumor extraction results of SSTS, FCM and MT with respect to the parameter settings in Table 1 based on mass and non-mass tumors respectively.

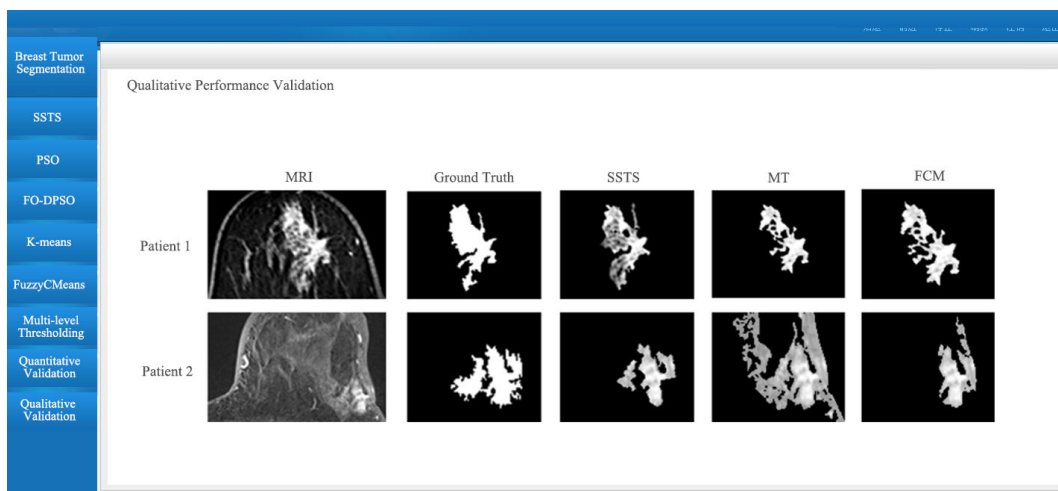


Fig. 4. Examples of tumor extraction results of SSTS, FCM, and Multi-level thresholding (MT) on MRIs of two patients: MRI of patient 1 contains a non-mass tumor, and MRI of patient 2 contains a mass tumor

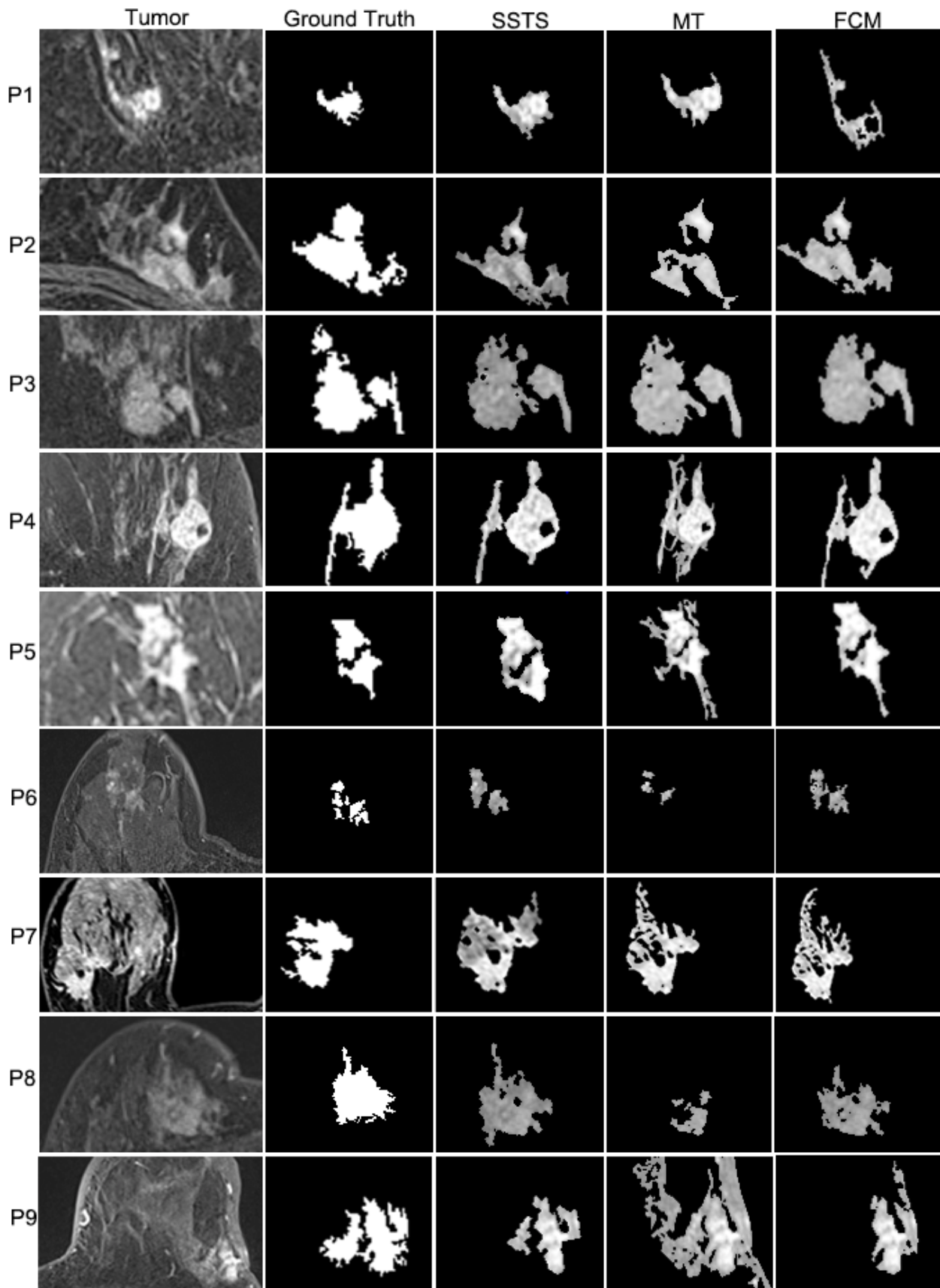


Fig. 5. Qualitative evaluation of Mass tumor extraction of MRIs of nine patients based on SSTS, FCM, and MT. The parameters of SSTS are set as: $\langle s; d; r \rangle = \langle 15; 5; 0.6 \rangle$

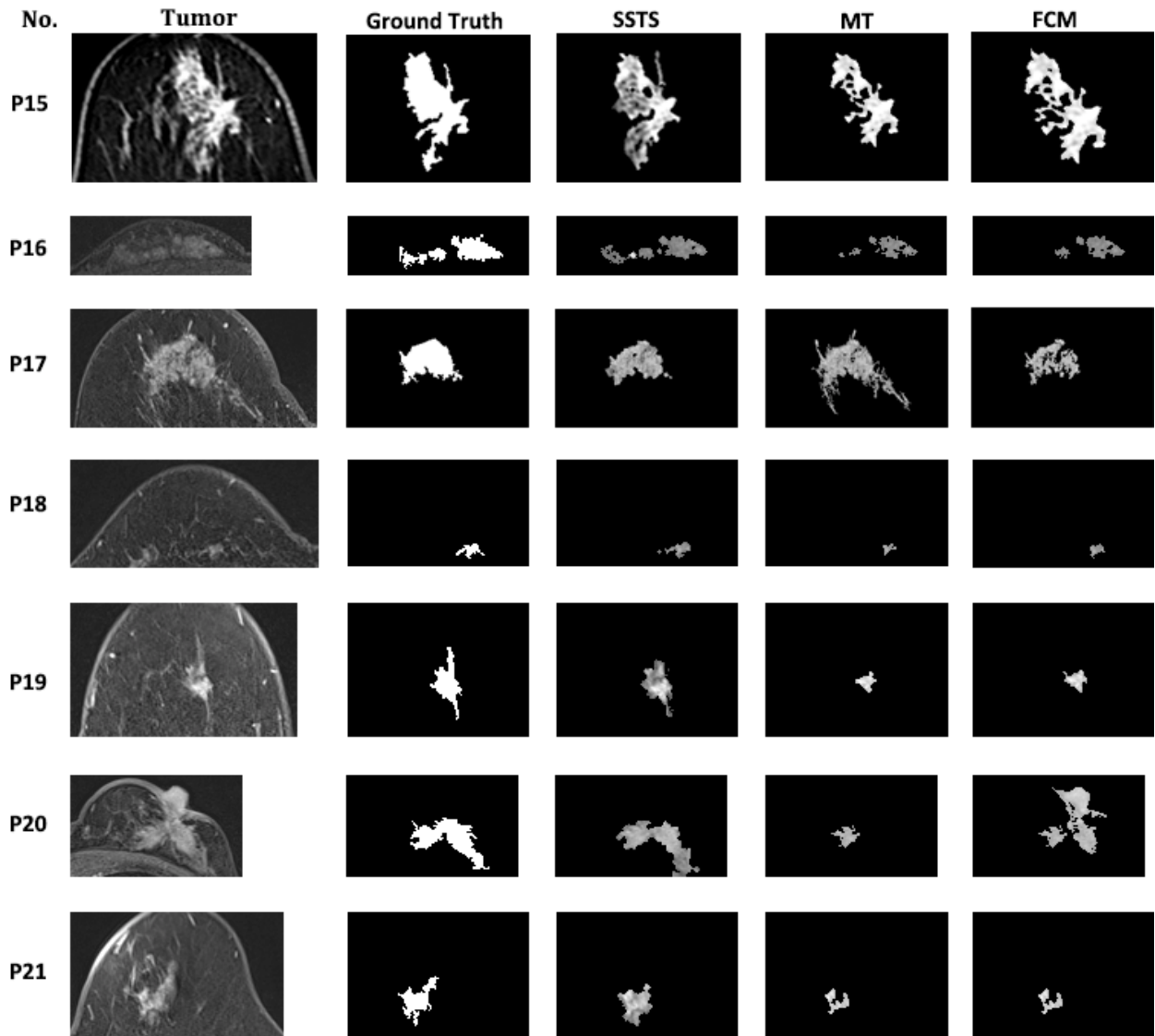


Fig. 6. Qualitative evaluation of Non-mass tumor extraction of MRIs of seven patients based on SSTS, FCM, and MT. The parameters of SSTS are set as: $\langle s; d; r \rangle = \langle 15; 5; 0.6 \rangle$

Meanwhile, the system shows the quantitative validation results between S and G by using five metrics: Dice Rate (DR), Precision (PR) and Recall (RC), which are defined in Table 1. We have initialized the parameter setting as the one resulting in an optimal performance based on the current dataset and parameter settings. The optimal settings and results are shown in Table 2, where $\langle s, d, r \rangle = \langle 15, 5, 0.6 \rangle$. Table 2 also quantitatively compares the performance of SSTS with the performance of FCM and MT, where the clustering number (cn) of FCM is 4, the separated level number of MT is 6, and $r = 0.6$ for classifier training of both FCM and MT.

Table 1. Definitions of validation metrics

Metrics	Formulas
DR	$\frac{2(S \cap G)}{S \cap G + S \cup G} * 100$
PR	$S \cap G / S$
RC	$S \cap G / G$

Table 2. Optimal parameter settings and segmentation results

Method	DR	PR	RC	para
SSTS	0.74	0.83	0.69	$\langle s, d, r \rangle = \langle 15, 5, 0.6 \rangle$
FCM	0.67	0.87	0.57	$\langle cn, r \rangle = \langle 4, 0.6 \rangle$
MT	0.67	0.85	0.6	$\langle ln, r \rangle = \langle 6, 0.6 \rangle$

From Table 2, the dice ratio and recall of SSTS are better than those of FCM and MT, while the precision of SSTS is worse than that of FCM and MT. Based on the definition of DR, PR, and RC (Table 1), the delineated area of SSTS tends to be larger than the true ground tumor area (ROI), while the FCM and MT tend to delineate an ROI's sub-area that cannot cover the whole tumor.

Our experiment is mainly based on MRIs containing tumors whose shortest radius are over 17 *pixels*. Fig. 7 shows two examples of tumors with short radius less than 17 *pixels* (namely very small tumors). The performance of SSTS based on very small tumors is not as efficient as its performance on normal tumors. The main reason is that the features textures of very small tumors cannot be described as well as the features of normal tumors, so it is difficult to distinguish the very small tumor area with the other parts in an MRI. How to efficiently extract very small tumors of MRIs will be our future work.

**Fig. 7.** Two examples of small tumors

3.4 SSTS System

Fig. 3 shows a screenshot of an MRI segmentation process of SSTS. Users can change parameter settings to see different segmentation results. The DB-patches are classified by a pretrained classifier with respect to a parameter setting (e.g. $s = 10$, $d = 10$, $r = 0.5$ in Fig. 5). Fig. 4 shows tumor extraction results of SSTS, FCM, and Multi-level thresholding (MT) of two patients: the MRI of patient 1 contains a non-mass tumor, while patient 2's MRI contains a mass tumor.

4 Conclusion

This paper presents an application of a set of image segmentation algorithms on segmenting IDC and DCIS tumors of Breast MRIs. Especially, it shows more advanced performance of SSTS for tumor extraction compared with other algorithms. The advantages of SSTS are its accuracy and flexibility of segmenting tumors based on adjustable parameters; and we have trained a set of classifiers with respect to different parameter settings for classifying tumor and non-tumor patches. However, the current parameter setting process is an exhaustive procedure, and only discrete parameter values are tested. Our future work will be on developing a more efficient parameter setting procedure; and extend our work to extracting more types of Breast tumors and very small tumors.

Acknowledgements

This paper is supported by the National Natural Science Foundation of China (Grants No. 61702274) and the Natural Science Foundation of Jiangsu Province (Grants No. BK20170958).

References

- [1] C. DeSantis, R. Siegel, P. Bandi, A. Jemal, Breast cancer statistics, 2011, CA: A Cancer Journal for Clinicians 61(6)(2011) 408-418.
- [2] W. Chen, M.L. Giger, U. Bick, A fuzzy c-means (FCM)-based approach for computerized segmentation of breast lesions in dynamic contrast-enhanced MR images 1, Academic Radiology 13(1)(2006) 63-72.
- [3] N. Gordillo, E. Montseny, P. Sobrevilla, State of the art survey on MRI brain tumor segmentation, Magnetic Resonance Imaging 31(8)(2013) 1426-1438.
- [4] X.-X. Yin, S. Hadjiloucas, J.-H. Chen, Y. Zhang, J.-L. Wu, M.Y. Su, Tensor based multichannel reconstruction for breast tumors identification from DCE-MRIs, PloS One 12(3)(2017), e0172111.
- [5] K. Nie, J.-H. Chen, J.Y. Hon, Y. Chu, O. Nalcioglu, M.-Y. Su, Quantitative analysis of lesion morphology and texture features for diagnostic prediction in breast MRI, Academic Radiology 15(12)(2008) 1513-1525.
- [6] A.B. Ashraf, S.C. Gavenonis, D. Daye, C. Mies, M.A. Rosen, D. Kontos, A multichannel Markov random field framework for tumor segmentation with an application to classification of gene expression based breast cancer recurrence risk, IEEE Transactions on Medical Imaging 32(4)(2013) 637-648.
- [7] N. Otsu, A threshold selection method from gray-level histograms, Automatica 11(285-296)(1975) 23-27.
- [8] P. Kovesi, Image segmentation using SLIC super-pixels and DBSCAN clustering. <<http://www.peterkovesi.com/projects/segmentation/>>, 2013 (accessed September 2017).
- [9] S. Kotsiantis, Combining bagging, boosting, rotation forest and random subspace methods, Artificial Intelligence Review 35(3)(2011) 223-240.
- [10] J. Kennedy, Particle swarm optimization, in: Encyclopedia of Machine Learning, Springer, Berlin, 2011, pp. 760-766.
- [11] P. Ghamisi, M.S. Couceiro, F.M.L. Martins, J.A. Benediktsson, Multilevel image segmentation based on fractional-order Darwinian particle swarm optimization, IEEE Transactions on Geoscience and Remote Sensing 52(5)(2014) 2382-2394.
- [12] X. Cai, F. Nie, H. Huang, Multi-view k-means clustering on big data, in: Proc. International Joint Conference on Artificial Intelligence, 2013.
- [13] M. Gong, Y. Liang, J. Shi, W. Ma, J. Ma, Fuzzy c-means clustering with local information and kernel metric for image segmentation, IEEE Transactions on Image Processing 22(2)(2013) 573-584.
- [14] S. Arora, J. Acharya, A. Verma, P.K. Panigrahi, Multilevel thresholding for image segmentation through a fast statistical recursive algorithm, Pattern Recognition Letters 29(2)(2008) 119-125.
- [15] D.C. Moura, M.A.G. Lopez, An evaluation of image descriptors' combined with clinical data for breast cancer diagnosis, International Journal of Computer Assisted Radiology and Surgery 8(4)(2013) 561-574.
- [16] L.-K. Soh, C. Tsatsoulis, Texture analysis of SAR sea ice imagery using gray level co-occurrence matrices, IEEE Transactions on Geoscience and Remote Sensing 37(2)(1999) 780-795.
- [17] A.K. Bhandari, V.K. Singh, A. Kumar, G.K. Singh, Cuckoo search algorithm and wind driven optimization based study of satellite image segmentation for multilevel thresholding using Kapurs entropy, Expert Systems with Applications 41(7)(2014) 3538-3560.
- [18] A. Bhandari, A. Kumar, G. Singh, Modified artificial bee colony based computationally efficient multilevel thresholding for satellite image segmentation using Kapurs, Otsu and Tsallis functions, Expert Systems with Applications 42(3)(2015) 1573-1601.

- [19] R.A. Husain, A.S. Zayed, W.M. Ahmed, H.S. Elhaji, Image segmentation with improved watershed algorithm using radial bases function neural networks, in: Proc. 16th International Conference on Sciences and Techniques of Automatic Control and Computer Engineering (STA), 2015.
- [20] J. Li, X. Li, B. Yang, X. Sun, Segmentation-based image copy move forgery detection scheme, IEEE Transactions on Information Forensics and Security 10(3)(2015) 507-518.
- [21] R. Girshick, J. Donahue, T. Darrell, J. Malik, Region-based convolutional networks for accurate object detection and segmentation, IEEE Transactions on Pattern Analysis and Machine Intelligence 38(1)(2016) 142-158.
- [22] I. Arganda-Carreras, S.C. Turaga, D.R. Berger, D. Ciros,an, A. Giusti, L.M. Gambardella, J. Schmidhuber, D. Laptev, S. Dwivedi, J.M. Buhmann, T. Liu, M. Seyedhosseini, T. Tasdizen, L. Kamentsky, R. Burget, V. Uher, X. Tan, C. Sun, T.D. Pham, E. Bas, M.G. Uzunbas, A. Carobna, J. Schindelin, H.S. Seung, Crowdsourcing the creation of image segmentation algorithms for connect-omics, Frontiers in Neuroanatomy 9(2015) 142.
- [23] Y. Yang, L. Guo, T. Wang, W. Tao, G. Shao, Q. Feng, Unsupervised multiphase color texture image segmentation based on variational formulation and multilayer graph, Image and Vision Computing 32(2)(2014) 87-106.
- [24] J. Yuan, D. Wang, R. Li, Remote sensing image segmentation by combining spectral and texture features, IEEE Transactions on Geoscience and Remote Sensing 52(1)(2014) 16-24.
- [25] M. Havaei, A. Davy, D. Warde-Farley, A. Biard, A. Courville, Y. Bengio, C. Pal, P.-M. Jodoin, H. Larochelle, Brain tumor segmentation with deep neural networks, Medical Image Analysis 35(2017) 18-31.
- [26] S. Pereira, A. Pinto, V. Alves, C.A. Silva, Brain tumor segmentation using convolutional neural networks in MRI images, IEEE Transactions on Medical Imaging 35(5)(2016) 1240-1251.
- [27] N. Sauwen, M. Acou, S.V. Caeter, D. Sima, J. Veraart, F. Maes, U. Himmelreich, E. Achten, S.V. Huffel, Comparison of unsupervised classification methods for brain tumor segmentation using multiparametric MRI, NeuroImage: Clinical 12(2016) 753-764.
- [28] A. Sehgal, S. Goel, P. Mangipudi, A. Mehra, D. Tyagi, Automatic brain tumor segmentation and extraction in MRI images, in: Proc. 2016 Conference on Advances in Signal Processing (CASP), 2016.
- [29] W. Chen, M.L. Giger, U. Bick, A fuzzy c-means (FCM) based approach for computerized segmentation of breast lesions in dynamic contrast-enhanced MR images, Academic Radiology 13(1)(2016) 63-72.
- [30] J. Li, X. Li, B. Yang, X. Sun, Segmentation-based image copy move forgery detection scheme, IEEE Transactions on Information Forensics and Security 10(3)(2015) 507-518.
- [31] Y. Zheng, B. Jeon, D. Xu, Q. Wu, H. Zhang, Image segmentation by generalized hierarchical fuzzy c-means algorithm, Journal of Intelligent & Fuzzy Systems 28(2)(2015) 961-973.
- [32] R.M. Haralick, K. Shanmugam, Textural features for image classification, IEEE Transactions on Systems, Man, and Cybernetics (6)(1973) 610-621.
- [33] Y. Freund, R.E. Schapire, Experiments with a new boosting algorithm, in: Proc. International Conference on Machine Learning 1996.
- [34] N.V. Chawla, K.W. Bowyer, L.O. Hall, W.P. Kegelmeyer, Smote: synthetic minority over-sampling technique, Journal of Artificial Intelligence Research 16(2002) 321-357.